Templating of Perovskite-Related Films Using Layer-by-Layer Assemblies and Nanoparticle Building Blocks

Erwan Geraud,* Helmut Möhwald, and Dmitry G. Shchukin

Max Planck Institute of Colloids and Interfaces, D-14424 Potsdam, Germany

Received July 27, 2007. Revised Manuscript Received May 26, 2008

Thin perovskite-related films have been obtained using a templating approach. First, nanoparticles of preformed hydroxide materials are synthesized by precipitation from the corresponding metal nitrates with ammonia solution. The resulting particles are then deposited layer-by-layer on glass substrate in alternation with oppositely charged polyelectrolytes. Two different techniques were used to realize the adsorption from nanoparticle suspension and polyelectrolyte solution: spraying and dipping. After removal of the polyelectrolyte template and formation of a perovskite-related layer by calcination, SEM characterization reveals thin flat films with morphology depending on the number of nanoparticle layers deposited. Homogeneous films are observed for one to three layers while they become inhomogeneous and contain big aggregates for thicknesses above five layers as a result of coarsening of smaller particles. The addition of adsorbed layers (from 1 to 15) results in an increase of the thickness (from 10 to 55 nm), but it appears that particles coarsen during thermal treatment and form large agglomerates that are then detached from the film, limiting the thickness increase. In addition to the short incubation time more perovskite-related material can be deposited when the spraying technique is used. The use of similar adsorption times in both spraying and dipping highlights the efficiency of spraying in terms of the deposited material.

Introduction

To enable new applications and improvement of material performance, the control of morphology is of great importance. One approach widely investigated is the templating method which can afford a fine control of the size, the shape, and the porosity of samples. For this various templates and templating procedures can be used. Depending on the applications, materials require a high degree of pore order and defined pore size, for optical devices, for example,[1,2] or can be used with irregular and polydisperse pores for separation or catalysis.[3]

The templating technique is used for the preparation of various structured materials as polymers, metal oxides, or metals. Their properties such as surface area, pore system, or size distribution of their composing particles are related to the organic template (polymer gels,[4,5] self-assembled block-copolymers,[6,7] polymer or silica beads[1]) and the overall structure is the replica of the initial template structure. The process allows the use of liquid or solid precursors as well as preformed nanoparticles[8] depending on the template nature and the reactions involved. Different structures like beads, microcapsules, or films have been built-up by the use of polyelectrolyte multilayers as template for nanoparticles.

Various metal oxide structures can be obtained using the templating method starting from sol−gel alkoxides or preformed nanoparticles as precursors.[9] In the sol−gel approach, the template is first impregnated by oxide precursor solutions, then the material is formed by hydrolysis and condensation reactions, and finally the template is removed either by dissolution or calcination. Concerning the use of nanoparticles, immobilization occurs by hydrogen bonding interactions as well as physical confinement.

Nanoparticles are particularly interesting precursors because of their availability and their small cost in comparison with sol−gel precursors; in addition, the morphology of the final material can be better controlled by changing the size and crystallinity of these particles.

Mixed metal oxides are of great interest as active oxide electrodes for the electrochemical reduction of oxygen in technological applications such as low temperature fuel cells, secondary metal−air batteries, and hydrogen production by water electrolysis, electrosynthesis, or catalysis.[10–15] The

* To whom correspondence should be addressed. E-mail: erwan.geraud@mpikg.mpg.de.

(1) Velev, O. D.; Kaler, E. W. *Adv. Mater.* **2000**, *12*, 7.
(2) Davies, M. E. *Nature* **2002**, *417*, 813.
(3) Tanev, P. T.; Chibwe, M.; Pinnavaia, T. J. *Nature* **1994**, *368*, 321.
(4) Caruso, R. A.; Giersig, M.; Willig, F.; Antonietti, M. *Langmuir* **1998**, *14*, 6333.
(5) Schattka, J. H.; Shchukin, D. G.; Jia, J.; Antonietti, M.; Caruso, R. A. *Chem. Mater.* **2002**, *14*, 5103–5108.
(6) Göltner, C. G.; Antonietti, M. *Adv. Mater.* **1997**, *9*, 431.
(7) Smarsly, B.; Polarz, S.; Antonietti, M. *J. Phys. Chem. B* **2001**, *105*, 10473–10483.
(8) Breulmann, M.; Davis, S. A.; Mann, S.; Hentze, H.-P.; Antonietti, M. *Adv. Mater.* **2000**, *12* (7), 502–507.
(9) Shchukin, D. G.; Caruso, R. A. *Adv. Funct. Mater.* **2003**, *13* (10), 789–794.
(10) Kinoshita, K. *Electrochemical Oxygen Technology*; Wiley: New York, 1992.
(11) Singh, R. N.; Lal, B. *Int. J. Hydrogen Energy* **2002**, *27*, 45–55.
(12) Bockris, J. O.; Otagawa, T. *J. Electrochem. Soc.* **1984**, *131*, 290–320.
(13) Sufredini, H. B.; Cerne, J. L.; Crnkovic, F. C.; Machado, S. A. S.; Avaca, L. A. *Int. J. Hydrogen Energy* **2000**, *25*, 415–423.
(14) De Chialvo, M. R. G.; Chialvo, A. C. *Electrochim. Acta* **1993**, *38*, 2442–2247.

10.1021/cm7020559 CCC: $40.75
Published on Web 08/02/2008

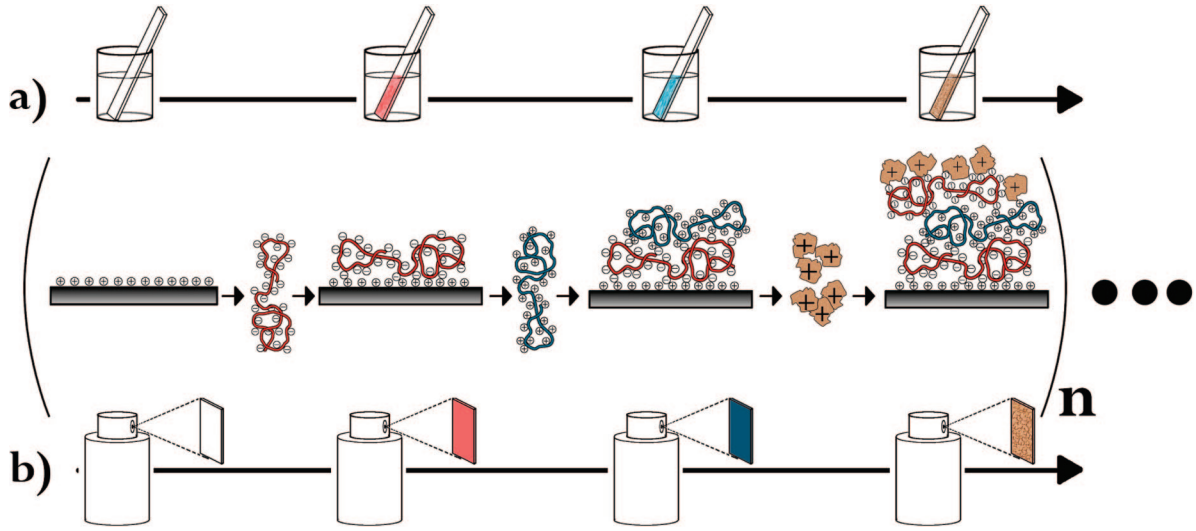

Figure 1. Schematic representation of the approach used to prepare nanostructured porous perovskite-related films.

copper-substituted lanthanum nickelates with a perovskite structure are promising candidates as electrodes for these processes, in particular as a cathode because of their mixed good oxygen-ion diffusivity and electronic conducting properties.[16–19] So, it is particularly interesting to synthesize them with a controlled morphology. In addition to the preparation of highly reactive surface materials with large surface area and optimized microstructure to avoid mass transport limitations during electrochemical reactions, research works are focused as well on the synthesis of new more active compositions for these oxides.[10]

In this paper, we report on the preparation of new perovskite-related ($La_2Ni_{0.8}Cu_{0.2}O_{4+\delta}$) films using a templating method. Perovskite materials have already been synthesized by a templating approach in polymer gel.[20] In this study, the films are built up by the layer-by-layer (LbL) technique consisting in adsorption of nanoparticles alternatingly with polyelectrolyte (PE) layers on the substrate surface (SiO_2). Preformed particles are first coated alternatingly with the negatively charged polyelectrolyte polystyrene sulfonate (PSS) and the positive one poly(allylamine hydrochloride) (PAH). In this case, polyelectrolyte multilayers act as a direct templating agent for perovskite-related nanoparticles. Two different adsorption techniques were employed for LbL deposition: spraying and dipping. The main advantage of the spraying technique is the very short time required to build the multilayer assembly. Previous works have shown that films obtained by dipping have a similar but nevertheless larger thickness than by spraying.[21] This can be explained by the fact that the short times used by spraying and the drainage on the surface do not allow newly absorbed layers to reach their equilibrium thickness. So, adsorption processes are different depending on the deposition technique and variations in properties of deposited layers and consequently the morphology of prepared films are expected. By this way, particles are homogeneously distributed and strongly stick to the surface allowing preparation of porous flat films and surface modification. Then, the polyelectrolyte multilayers were removed by thermal treatment in air. This step permits the use of metal salts or hydroxide nanoparticles as starting materials, since they can be converted into oxides during calcination. The proposed approach allows fabrication of perovskite-related nanostructured films with nanoscale precision on the surface of various templates, as well as on bulk perovskite structures (dense perovskite pellets).

Experimental Section

Materials. Sodium poly(styrene sulfonate) (PSS, Mw ~70 000), poly(allylamine hydrochloride) (PAH, Mw ~ 70 000) were obtained from Sigma-Aldrich Co. (U.S.A.). For nanoparticle preparation lanthanum nitrate hexahydrate and nickel nitrate hexahydrate were purchased from Fluka, and copper nitrate trihydrate was obtained from Alfa Aesar. The precipitating agent, ammonia aqueous solution, was purchased from Fluka. The water used in all experiments was prepared in a three stages Millipore Milli-Q Plus 185 purification system and had a resistivity higher than 18 MΩ·cm.

Synthesis of Initial Nanoparticles and Layer-by-Layer Assembly. The initial oxide nanoparticles have been prepared by precipitation of the mixture of metal nitrates in the presence of ammonium hydroxide solution. First, nitrate precursors are dissolved in water (20 mL) with respect to the stoichiometry, that is, in the following concentrations: 1.25 M for $La(NO_3)_3$, 0.5 M for $Ni(NO_3)_2$, and 0.125 M $Cu(NO_3)_2$ for the expected composition $La_2Ni_{0.8}Cu_{0.2}O_{4+\delta}$. Then, ammonia solution (2.5%) is added dropwise to the nitrates solution under vigorous stirring. Starting from 200 μL the solution becomes turbid and the addition is pursued until the pH reach 9.5. Finally, the as-synthesized particles are washed with water by three centrifugation (5000 rpm, 5 min)−redispersion cycles.

(15) Hu, C. C.; Lee, Y. S.; Wen, T. C. *Mater. Chem. Phys.* **1997**, *48*, 246–254.
(16) Mauvy, F.; Boehm, E.; Bassat, J.; Grenier, J.; Fouletier, J. *Solid State Ionics* **2007**, *178*, 1200–1204.
(17) Kharton, V. V.; Yaremchenko, A. A.; Tsipis, E. V.; Frade, J. R. *Solid Oxide Fuel Cells VIII (SOFC VIII)* **2003**, 561–570.
(18) Kharton, V. V.; Tsipis, E. V.; Yaremchenko, A. A.; Frade, J. R. *Solid State Ionics* **2004**, *166*, 327–337.
(19) Boehm, E.; Bassat, J. M.; Steil, M. C.; Dordor, P.; Mauvy, F.; Grenier, J. C. *Solid State Sci.* **2003**, *5*, 973–981.
(20) Shchukin, D. G.; Yaremchenko, A. A.; Ferreira, M. G. S.; Kharton, V. V. *Chem. Mater.* **2005**, *17*, 5124–5129.
(21) Izquierdo, I.; Ono, S. S.; Voegel, J.-C.; Schaaf, P.; Decher, G. *Langmuir* **2005**, *21* (16), 7558–7558.

Multilayers of polyelectrolytes and nanoparticles have been assembled using the initially preformed nanoparticles by two approaches (Figure 1). In both cases, film fabrication consists in depositing alternatingly on substrate surfaces differently charged (positive and negative) polyelectrolyte solutions and particles from suspensions. By this way the particles are trapped between polyelectrolyte layers and fixed to the substrate. In our case microscope glass slides are used as a model substrate. Glass slides are cleaned by ethanol and soaked in Piranha solution for 15 min and in a cleaning solution (H_2O:NH_4OH:H_2O_2, 1:1:5) for 15 min at 75 °C followed by drying under a nitrogen stream before the use. Particle suspensions were used at a mass concentration of 1%, and their dynamic viscosity is 0.9 mm^2/s.

The first adsorption method consists in dipping the substrates into polyelectrolyte solutions and into particle suspension in water (Figure 1a). Layers are obtained by immersing a cleaned substrate alternatingly in 2 mg/mL oppositely charged polyelectrolyte solutions containing 0.5 M NaCl. The withdrawal rate is 2 cm/s downward and 3 cm/s upward. The incubation times used are 15 min in the polyelectrolyte solutions and 30 min in the particle suspension (0.15 mg/mL).

Between each adsorption step the substrate is cleaned by immersion in water. The adsorption sequence consists in first adsorbing a bilayer of PSS and PAH to increase adhesion and to achieve homogeneous surface coverage followed by consecutive adsorption of PSS and positively charged nanoparticles. This PSS/PAH/PSS/nanoparticles sequence was repeated from 1 up to 50 times to build the film and to achieve films with variable thickness and surface morphology.

An alternative assembly route is based on the spraying (Figure 1b) of the polyelectrolyte solutions and nanoparticle suspensions onto the surface of the substrate. PSS/PAH multilayer films were built on a first PEI layer ensuring strong adhesion of the next layers to the substrate. This PEI layer was deposited by dipping (2 mg/mL, 0.5 M NaCl) using a contact time of 20 min. After PEI was absorbed, the films were built-up by spraying polyelectrolyte solutions and nanoparticle suspension using spray cans purchased from Roth. The spraying times for polyelectrolytes were 3 s followed by 27 s of contact, and these times were respectively 6 and 24 s for particle suspension. The spraying distance to the target is 10 cm, and the spraying rate is 40 mL/min.

After each adsorption step substrates were washed by spraying water during 20 s. For both spraying and dipping, the last preparation step consists of drying assembled multilayer films under nitrogen stream.

It has been shown in previous work[21] that, by spraying, the thickness of the adhered suspension is very thin and the drainage is very fast, so the concentrations in the spray cans and in the adhering films are identical. That means that short contact times are needed. On the opposite, by dipping, the depletion zone formed at the deposition surface is playing an important role and longer times are required.

The removal of the organic polyelectrolyte multilayers and the formation of structured perovskite-related films were performed by calcination at 500 °C. Polyelectrolyte/nanoparticle films on SiO_2 substrate are placed in a furnace and heated under nitrogen flow during temperature ramping to 500 °C (1 h) to allow particle sintering in the presence of organic matter, then nitrogen is replaced by air (1 h) to permit removal of polyelectrolyte template multilayers and synthesis of perovskite-related material.

Characterization

Wide angle X-ray scattering (WAXS) was performed using an Enraf-Nonius PDS-120 apparatus. The size and ζ-potential of particles were determined by a Nano-ZS Zetasizer from Malvern instruments. The morphology of the prepared films was examined using scanning electron microscopy (SEM) with Gemini Leo 1550 apparatus.

The LbL film growth by deposition of nanoparticles in alternation with PSS and PAH was followed in situ by using a Q-Sense E4 quartz crystal microbalance (QCM) in a liquid-cell setup. A layer of poly(ethylenimine) (PEI) was first adsorbed from a 2 mg/mL PEI solution containing 0.5 M NaCl. In the measurements, the polyelectrolyte solutions and particle suspensions were flowed for 5 and 10 min, respectively, and left in contact with the electrode for 10 min. After adsorption a washing step was performed with Milli-Q water for 5 min. The resonators used were gold electrodes coated with evaporated silica (ca. 50 nm thick) to increase the efficiency and to achieve the same adsorption conditions as for the initial SiO_2 support.

To estimate the thickness of the obtained perovskite-related films, the samples were embedded in poly(methyl metacrylate)m and then ultrathin sections (30−100 nm in thickness) were obtained using a Leica ultracut UCT ultramicrotome. Carbon-coated copper grids were used to support the thin sections, and a Zeiss EM 902A transmission electron microscope (TEM) was employed for analysis. XPS analysis of the composition of the samples was performed using an AXIS Nova X-Ray photoelectron spectroscope from Kratos Analytical.

Results and Discussion

Preformed oxide nanoparticles have a positive zeta potential of approximately 45 mV. Characterization of as-synthesized particles by dynamic light scattering evidences a bimodal size distribution. The two main particle diameters are 150 and 600 nm; they correspond to agglomerates of smaller elongated particles (around $60 \pm 20 \times 300 \pm 100$ nm according to SEM analysis). The average size and the size distribution can be partially reduced by use of ultrasound treatment for a short time, 1−5 min, a longer time inducing increase of particle size by coarsening.[22] The high collision speeds associated to the very high temperature created by the intense sound waves induce local melting and then aggregation. A change in solution color from light blue to brown can be attributed to the formation of some oxides by reaction with air, promoted by ultrasound treatment.

According to XRD (see Figure 2), initially prepared particles contain different phases like copper nitrate hydroxide and probably other metal hydroxides, and the latter is not crystallized enough to be clearly identified. The low crystallinity does not allow the determination of the crystallite size from the XRD patterns.

Multilayer assemblies have been built from these nanoparticles and the polyelectrolytes PAH and PSS, the number of deposited layers of nanoparticles varying between 1 and 15. By quartz crystal microbalance (QCM) measurements (Figure 3) it has been possible to follow directly the increase of the film mass with the number of layers deposited. Each polyelectrolyte layer deposition induces a decrease of the frequency due to the increase of the adsorbed material mass. After contact with a particle suspension, a small frequency decrease is observed, which means that only a small amount of particles was deposited on the electrodes and/or a part of

(22) Suslick, K. S. *Sci. Am.* **1989**, *260*, 80–8.

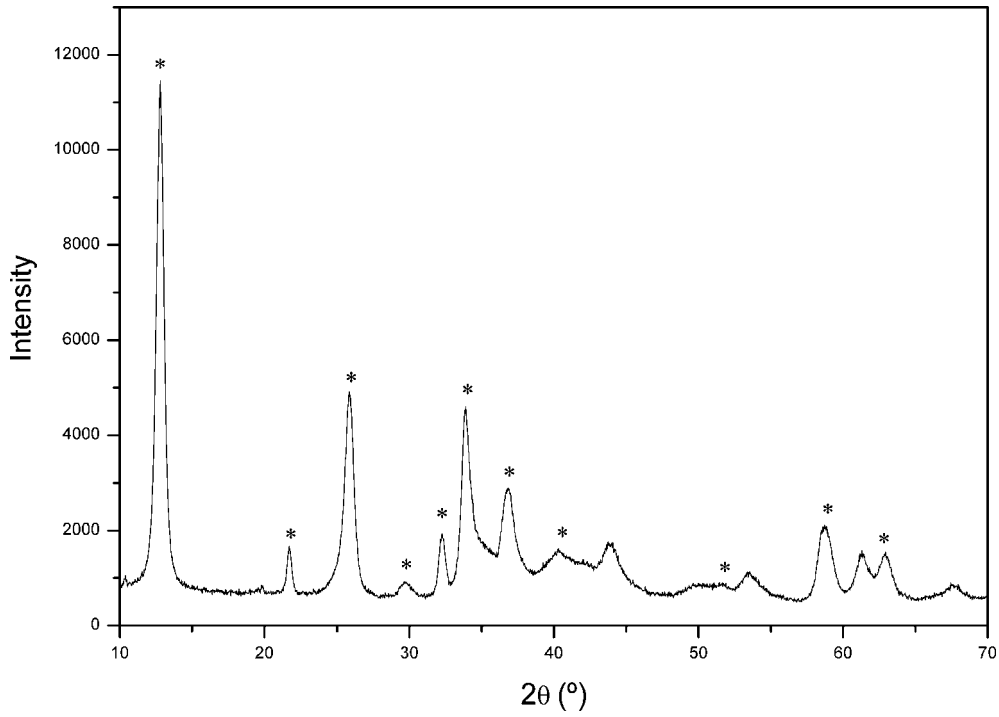

Figure 2. XRD patterns of the initial as-prepared nanoparticles. Peaks correspond mainly to copper nitrate hydroxide (stars) and a mixture of nickel and lanthanum hydroxides or nitrate hydroxides.

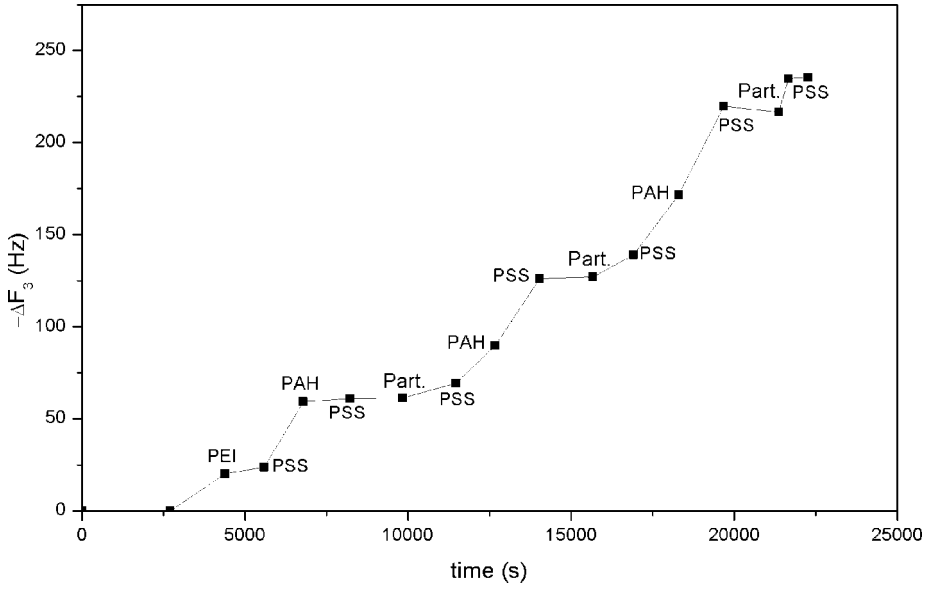

Figure 3. Monitoring of layer-by-layer assembly of polyelectrolytes and preformed nanoparticles by QCM measurements on SiO_2 coated gold electrodes.

the polyelectrolyte has been desorbed. The subsequent decrease of the frequency when PSS is flowing indicates an increased sorption of the polyelectrolyte and by this way an effective adsorption of particles.

After assembly of multilayers we removed the polyelectrolyte template film in order to obtain a thin coating of nanostructured perovskite-related material. After calcination, the XRD pattern (Figure 4) displays narrow peaks; nevertheless, an increased peak width indicates that the perovskite-related material after calcination possesses a nanoparticulated structure. The pattern is similar to the one recorded on the $La_2(Ni,Cu)O_4$ solid solutions synthesized via Pechini route before high temperature calcination. At this temperature (500 °C) the structure is close to La_2CuO_4,[23] and indeed the formation of the K_2NiF_4-type (perovskite related) structure requires calcination above 700 °C. XPS analysis of the products after calcination of the polyelectrolyte template and formation of the oxide yields the composition $La_{1.90}Ni_{0.90}Cu_{0.25}O_{4+\delta}$, which is very close to the composition expected, however with an excess of nickel and copper.

As shown in the SEM pictures in Figure 5, samples after calcination of the template present a thin layer of coarsened nanoparticles (bright areas) approximately 50 nm in diameter

(23) Zhu, Y.; Tan, R.; Yi, T.; Gao, S.; Yan, C.; Cao, L. *J. Alloys Compd.* **2000**, *311*, 16–21.

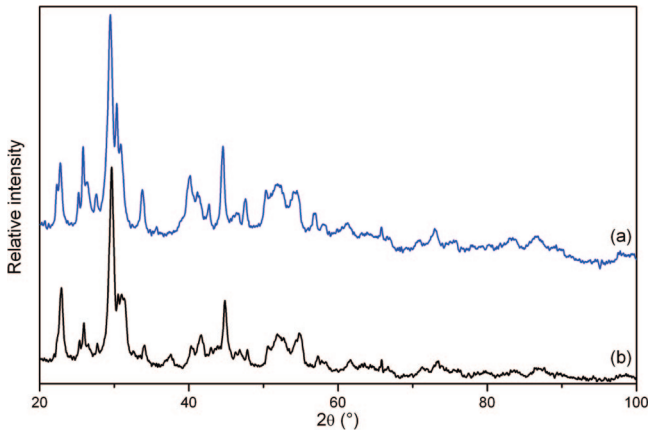

Figure 4. XRD pattern of the resulting structured perovskite-related film after template removal by calcination at 500 °C under air (a). The XRD pattern presents signals of a standard $La_2Ni_{0.8}Cu_{0.2}O_{4+\delta}$ material prepared via the Pechini route (b). The increased width of the signals indicates nanoparticulate structure of the perovskite-related film.

that stick to the glass substrate for both dipping deposition and spraying. While a homogeneous flat surface containing breaks is obtained when dipping is used, by spraying, bigger aggregates are present, smaller cracks are observed, and the film is denser. These results suggest that by spraying a higher amount of material is deposited.

SEM pictures of the resulting calcined films are displayed in Figure 6. For one layer of particles deposited by dipping, the images evidence homogeneous and flat films composed of a layer of small coarsened particles approximately 50 nm in size and of few bigger ones (ca. 100 nm) on the top. By spraying, films are similar, but more big aggregates (100−500 nm) are observed on the top than for films obtained by the dipping process.

Increasing the number of deposited particle layers to three leads to identical observations (not shown), that is, regular flat surfaces composed of small particles with some additional big particles when spraying is used. No noticeable differences of the film morphology have been observed between the two techniques for a small number of deposited layers of the initial oxides.

When the number of layers is increased to five for both dipping and spraying deposition, inhomogeneous films are observed: a thin layer of small coarsened particles is still observed but bigger particle aggregates with sizes from 100 nm to 10 μm are distributed randomly. With dipping, the majority of the large particles after calcination have a needle shape arranged to form stars, while with spraying these crystallites are isolated. As expected, the size of the observed particles increases with the number of layers. Films prepared with 15 layers of nanoparticles adsorbed by dipping contain a thin layer of small particles, bigger ones of approximately 100 nm are randomly dispersed, and also some very big aggregates up to 100 μm can be found (not shown).

The sprayed films do not display such micrometer-scale particle aggregates after calcination and consist only of a thin layer of small particles and bigger ones (100−300 nm) on the surface. We suppose that this morphology is due to the fact that the very big agglomerates formed during thermal treatment by coarsening of smaller particles are detached from the substrate surface after calcination because of their large size and small interaction with the thin perovskite-related layer. The larger the amount of deposited inorganic material, the bigger are the aggregates after sintering, which can be an explanation for the absence of very big particles when spraying is used. The projection of particles by spraying can allow the adhesion of a bigger particle than by dipping, and more deposited material is available to form big aggregates.

The increase of deposited nanoparticle layer thickness induces an increase of material amount at the substrate surface as shown by QCM measurements. Considering the fact that the polyelectrolyte template removal by calcination induces coarsening of particles, we suppose that part of the final material is detached from the glass surface after forming big aggregates. This effect explains the differences observed when we compare spraying and dipping. For small numbers of layers coarsened particles or aggregates are bigger when spraying is used because of the larger amount of particles deposited. For a big number of nanoparticle layers (15), aggregates become too large to stick and are detached from the surface of the samples prepared by spraying, while the samples prepared by dipping still display large agglomerates. For a big number of particle layers big aggregates are also formed, but their adhesion energy scales only with radius and they can be easily removed by other forces.

Because of the small thickness of the films it is not possible to measure directly the porosity. If we look closely at the films obtained by dipping (Figure 7), it appears that when the layer number is increased, here from 5 to 50, the films look denser and contain bigger cracks.

As mentioned in the experimental section, longer contact time is required when dipping is used in comparison with spraying. When particle suspensions are used instead of polyelectrolyte solutions, adsorption process and kinetics can be modified, so additional dipping experiments have been realized with short adhesion times similar to the ones used for spraying (contact time = 1 min). As expected, it seems that less material is deposited on the surface (Figure 8). The calcined films are formed by particles aggregated to make a network. The porosity is much more open if compared with the slow dipping process. In this case the dipping time is not long enough to reach the equilibrium and permit the adhesion of the particles at the substrate surface.

The average thickness of the deposited films after calcination was estimated by TEM analysis of the ultramicrotomed samples. As seen in Figure 9, the tendency to increase the thickness (average thickness of the porous nanostructured films excluding randomly situated big aggregates) increases with the number of deposited nanoparticle layers for both dipping and spraying deposition. However, the thickness of the film obtained by spraying is approximately 1.5−2 times larger than for the films produced by the dipping method regardless of the number of deposited nanoparticle layers, which coincides with other observations confirming the formation of thicker layers by spraying. Linear growth of the thickness with increasing layer number is not observed for both deposition methods; the films exhibit continuous reduction of the growth increment with higher numbers of

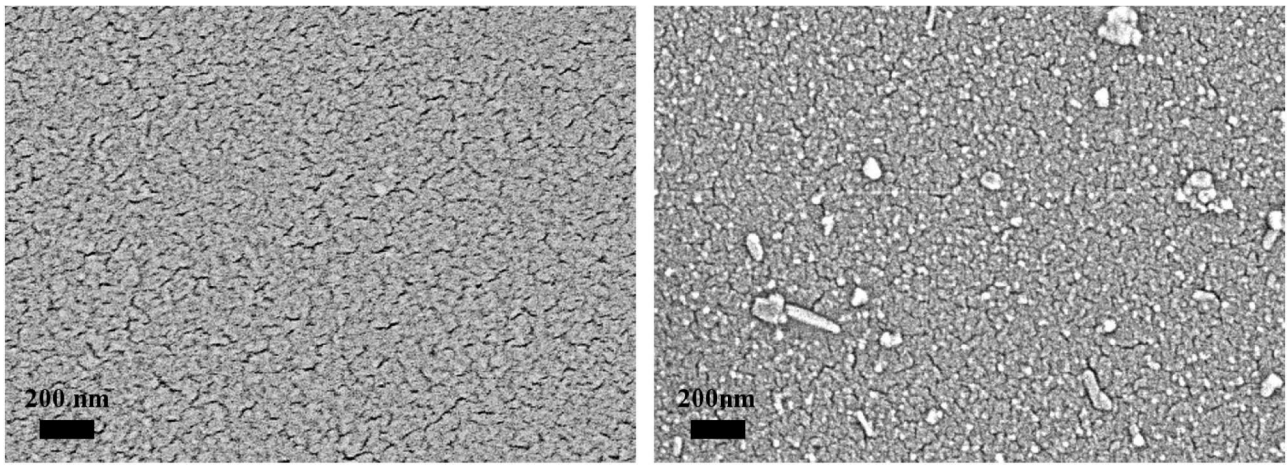

Figure 5. Close SEM views of samples prepared by dipping (left) and by spraying (right).

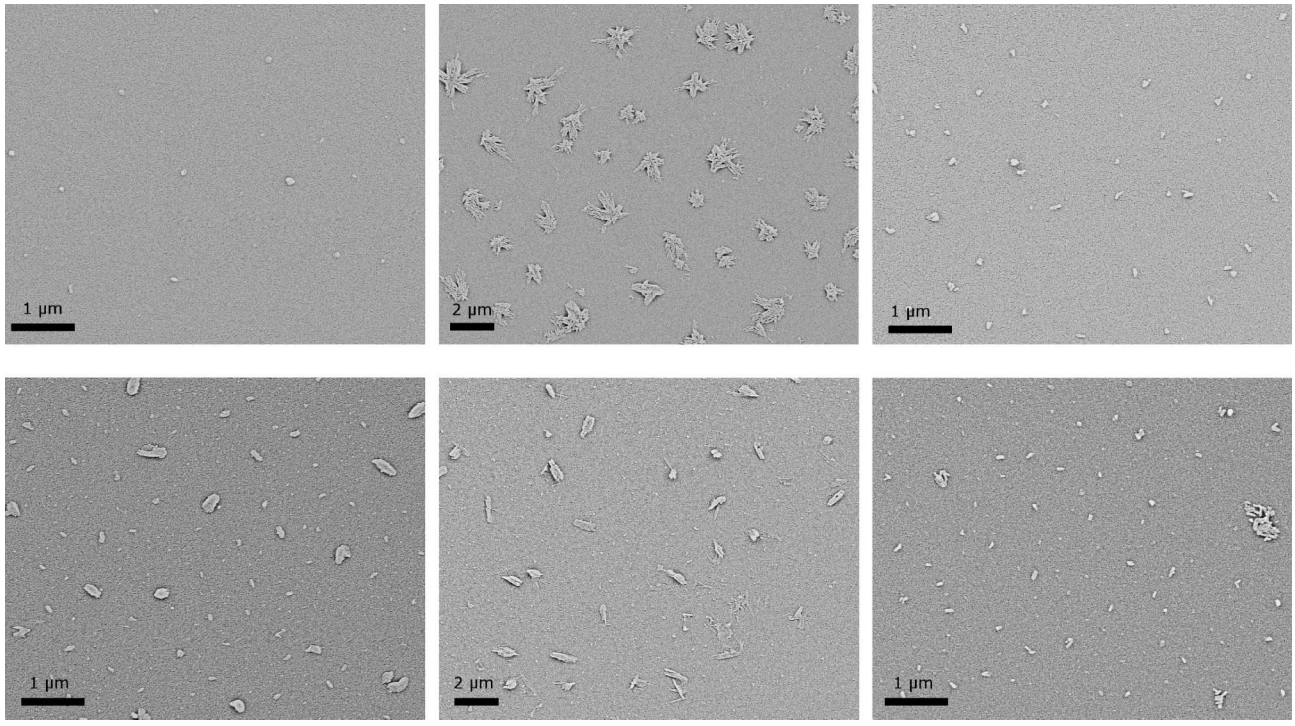

Figure 6. SEM pictures of samples prepared by dipping (on top) and by spraying (bottom) for different numbers of layers (1, 5, and 15 from left to right).

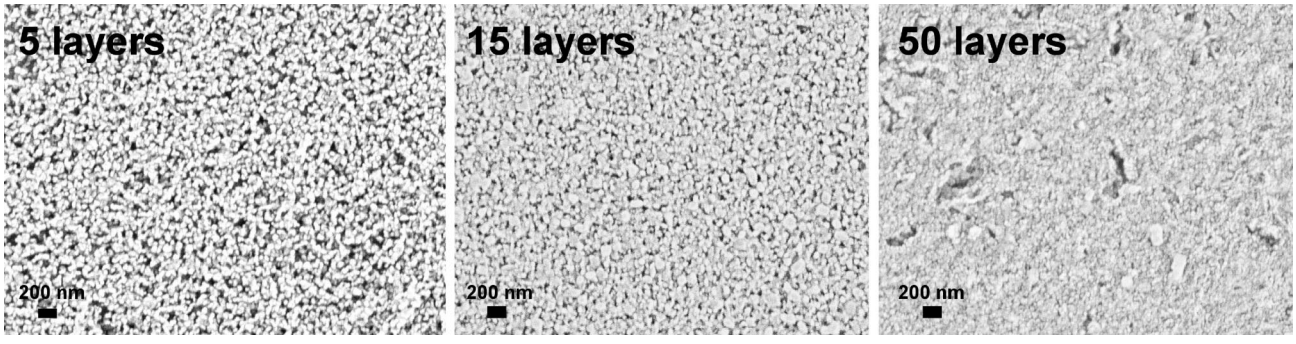

Figure 7. SEM pictures of samples prepared by slow dipping for different numbers of layers (5, 15, and 50 from left to right).

deposited layers, which supports the above-mentioned idea of enhanced aggregation of the particles followed by detachment of the aggregates from the film upon calcination when more perovskite-related material is deposited onto the template polyelectrolyte multilayers. Such a growth behavior allows one to conclude the existence of the maximal critical thickness of the calcined nanostructured porous perovskite-related film obtained by the layer-by-layer assembly ap-

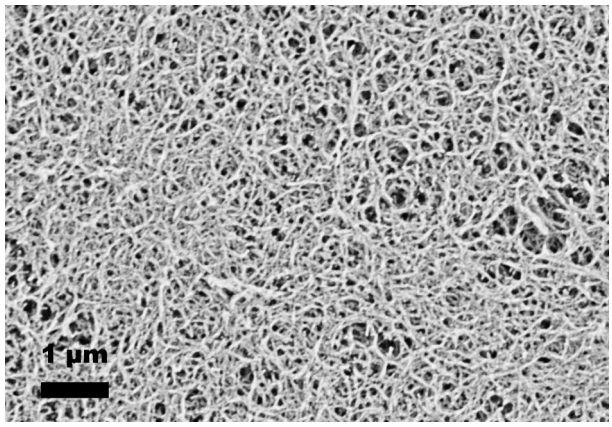

Figure 8. SEM picture of a film obtained by fast dipping for 15 layers.

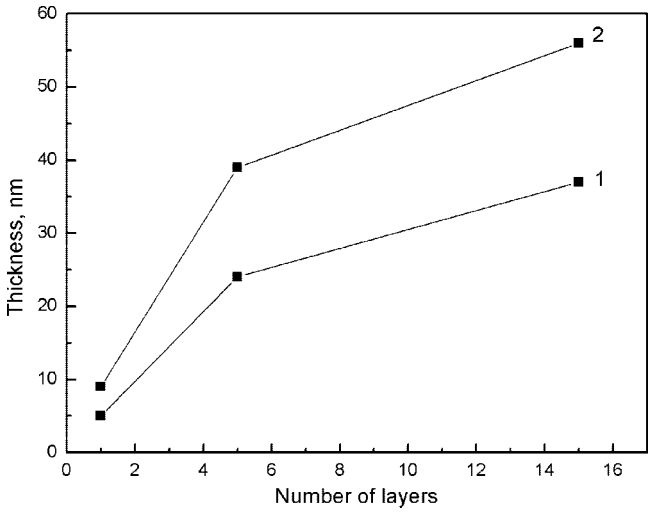

Figure 9. Evolution of the film thickness from slow dipping (1) and from spraying (2) measured after calcination by TEM analysis of ultramicrotomed samples.

proach, which cannot be exceeded by the further deposition of additional nanoparticle/polyelectrolyte multilayers.

In our case the spraying method, in addition to the advantage of the short time required, permits more material to be deposited and to have a rougher surface. According to the literature, polyelectrolyte films prepared by spraying are thinner than by dipping,[21] but in our case the resulting inorganic films obtained by spraying contain more material. Short contact times, similar to the ones used by spraying, lead to even thinner films when dipping is used. The results presented could be of interest for applications such as electrodes (cathode) in solid oxide fuel cells, since in this field it is interesting to prepare flat films having sufficient roughness and a big surface area to improve the reactivity.

Conclusion

The preparation of perovskite-type material was performed using a templating approach that consists of adsorption of polyelectrolytes in alternation with nanoparticles of preformed hydroxide materials. Preformed nanoparticles can be obtained simply by coprecipitation with ammonia solution from the corresponding salts. After calcination, the organic template is removed and hydroxides are converted into perovskite-related material. The resulting nanostructured porous films display quite homogeneous flat surfaces for one to three deposited layers of particles. Above five layers, inhomogeneous films are observed and big aggregates are present as a result of coarsening of smaller particles. For fifteen layers of particles few materials remained on the substrate probably due to the formation of big aggregates that cannot stick on the surface.

Both methods, spraying and dipping, can be used, but spraying appears to be the more efficient way in terms of time and quantity of deposited material. In the case of dipping, the equilibrium is not reached when short adsorption times are used; as a result less material is deposit on the surface and more porous films are obtained. These results show the possibility to prepare thin nanoparticulated porous films of perovskite-type materials and allow preparation of nanostructured films having a high reactivity on different substrates.

Acknowledgment. Financial support from the European MatSILC Project is gratefully acknowledged.

CM7020559